Journal of Renewable Materials

Tech Science Press

DOI: 10.32604/jrm.2022.019821

ARTICLE

Utilization of Dredged River Sediment in Preparing Autoclaved Aerated Concrete Blocks

Kai Zhang[1,2], Qunshan Wei[1,2,*], Shuai Jiang[3], Zhemin Shen[4], Yanxia Zhang[1,2], Rui Tang[1,2], Aiwu Yang[1,2] and Christopher W. K. Chow[5]

[1]College of Environmental Science and Engineering, Donghua University, Shanghai, 201620, China

[2]State Environmental Protection Engineering Center for Pollution Treatment and Control in Textile Industry, Donghua University, Shanghai, 201620, China

[3]National Engineering Research Center of Dredging Technology and Equipment, Shanghai, 200120, China

[4]School of Environmental Science and Engineering, Shanghai Jiao Tong University, Shanghai, 200240, China

[5]Scarce Resources and Circular Economy (ScaRCE), UniSA STEM, University of South Australia, Mawson Lakes, SA 5095, Australia

[*]Corresponding Author: Qunshan Wei. Email: qswei@dhu.edu.cn

Received: 17 October 2021 Accepted: 17 January 2022

ABSTRACT

In this study, the dredged river sediment, soft texture and fine particles, is mixed with other materials and transformed into eco-friendly autoclaved aerated concrete (hereinafter referred to as AAC) blocks. The results indicated the bricks produced under the conditions of 30%–34% dredged river sediment, 24% cement, 10% quick lime, 30% fly ash, 2% gypsum and 0.09% aluminum powder with 0.5 water to material ratio, 2.2 MPa autoclave pressure and 6 h autoclave time, the average compressive strength of 4.5 MPa and average dry density of 716.56 kg/m^3 were obtained, the two parameters (strength & density) both met the requirement of national industry standard. At the same time, the contents of dredged river sediment, cement, lime, fly ash, gypsum and aluminum powder were 15%, 48%, 20%, 15%, 2% and 0.09%, respectively, and the non-AAC block made of 0.5 water to material ratio, the average compressive strength of 3.1 MPa and average dry density of 924.19 kg/m^3 were obtained, the two parameters (strength & density) also met the requirement of national industry standard. In addition, the AAC block's phase composition and morphology were micro-analyzed by SEM and XRD, the main substances in AAC block were found to be tobermorite and CSH, Among them, the chemical bond between Si-O-Si and Al-O-Al is broken, Al-O-Si is regenerated, Al substituted tobermorite with better strength is formed, and the compressive strength of AAC is further improved.

KEYWORDS

Autoclaved aerated concrete; dredged river sediment; compressive strength; frost-resistance; moisture content; microstructure

1 Introduction

The rapid development of urbanization introduces serious urban river pollution issues. Rainwater runoff with heavy metals, carbonate substances and contaminants, such as air settlement (dust, sulfur oxide, nitrogen oxide, etc.), industrial, agricultural and domestic sewage discharge (heavy metal, COD, BOD,

etc.), can enter the waterway by different channels [1–3]. These pollutants can be transformed into solid through physical and chemical actions, and then deposited in the dredged river sediment, which leads to a serious dredged river sediment pollution issue [4]. Li et al. studied the tidal flat near Yuantuojiao in the North Branch of the Yangtze River Estuary and found that the average content of heavy metals, Co and V, was significantly higher than the background value, except Cr and the other six elements Zn, V, Ni, Co, Cu and Mn which are in a group of high human contribution rate, which concluded the environmental factors would affect the distribution of sediments and then affect the distribution of heavy metals [5]. At present, there are two main methods to treat dredged river sediment, namely *in-situ* disposal and off-site disposal [6]. *In-situ* disposal refers to the direct application of physical, chemical, or biological technology to the sediment in the river without dredging, to reduce the amount of polluted dredged river sediment or release the toxicity of pollutants in the sediment [7]. At this stage, many in-situ disposal technologies of dredged river sediment, including chemical remediation technology, plant remediation technology, microbial remediation technology, in-situ masking, apply oxidant, and combined remediation technology, such as chemical/biological and microbial/plant, etc., can be found [8]. Chao et al. found that biochar can significantly reduce the bioavailability of metals (except Cr) in pore water, thus reducing the uptake of heavy metals by river benthos [9]. While in-situ disposal technology is not mature and still suffers from the potential damage of the river ecology. Therefore, the current most used treatment of dredged river sediment is mainly applying off-site treatment technology. That is, after dredging the dredged river sediment, dig out the sediment and then burn it (incineration) or dispose of it as a landfill [10,11]. In recent years, due to the introduction of resource management, treatment of dredged river sediment has gained more attention, which can be made into new products, such as filling and building materials by physical and chemical means [12]. Due to the soft texture, small particle size, high water content, and large volume of dredged river sediment, therefore, it has not been considered in the as a raw material for building and construction materials. In addition, aerated concrete can also be used for multiple purposes. He et al. used aerated concrete waste after wet grinding as a substitute cementing material in cement and concrete [13]. Jin et al. [14] found that AACW can be reused as fine aggregate for internal solidification. The addition of AACW can also refine the pore structure of cement mortar, increase the ratio of harmless pores and less harmful pores, and increase the interfacial transition zone micro-hardness around the porous material.

AAC block is a new type of lightweight building material, usually made of calcareous or siliceous materials as the main body, after adding foaming agent and additives through the process of batching, dry wet mixing, pouring, curing, demoulding, cutting, steaming. It has excellent performance and with the benefits of light weight, good compression resistance, heat preservation and fire protection, good frost resistance, and has good energy saving and emission reduction effect in the process of production and application. It is a good environmentally friendly product in response to the national sustainable development policy and has a good market development prospect [15]. Zuhair et al. used construction solid waste to prepare AAC blocks [16]. Cai et al. [15,17] used red gypsum instead of fly ash to prepare the AAC block. Its dry density and compressive strength meet the requirements of B06 and A3.5 in ***GB/T 11968-2006 autoclaved aerated concrete block***. Peng et al. used graphite tailings as silica material to prepare AAC block, and successfully prepared the dry density of 666 kg/m^3 and AAC with compressive strength of 5.0 MPa [18]. In addition, aerated concrete can also be used twice. He et al. used aerated concrete to dismantle waste after wet grinding, which can be effectively used as a substitute cementing material in cement and concrete [13]. Yang et al. found that AACW can be broken instead of fine aggregate for internal solidification. The addition of AACW can also refine the pore structure of cement mortar, increase the ratio of harmless pores and less harmful pores, and increase the interfacial transition zone micro-hardness around the porous material [14].

At present, using dredged river sediment to prepare backfill materials and building materials is a hot spot in the treatment of dredged sediment. Wang et al. [19] used dredged river sediment, bentonite, and zeolite as additives in a certain proportion, and sintered large pore lightweight ceramsite , which can be used in water treatment systems. Chen et al. [20] synthesized a ceramsite with excellent adsorption performance to treat Pb (II) polluted wastewater, using biomass and sewage sludge ash (CBSA), fly ash gasification (GCFA), and sewage sludge (SS) as raw materials. Slimanou et al. [21] used a large amount of dredged river sediment generated by port activities to prepare sintered bricks. The proportion of dredged river sediment and sintering temperature are the two main factors that determine the quality of sintered bricks. Yet the current utilization of dredged river sediment mainly focuses on the preparation of ceramsite and aggregate, while the research on the preparation of AAC block with dredged river sediment is less [12].

This paper describes how to prepare AAC block from dredged river sediment, and test its dry density, compressive strength, freeze-thaw property and heavy metal leaching content. It has broad application value and prospect as a new light building material. In this paper, the AAC block prepared from dredged river sediment can not only realize the resource utilization of dredged river sediment, but also reduce the environmental pressure and realize the unity of environmental, social and economic benefits. The resource comprehensive utilization of solid waste is an important part of the development of the Chinese environmental industry, which has a certain practical research significance [22].

2 Material and Methods

2.1 Materials and Agents

The dredged river sediment was collected from a river in Jiaxing, Zhejiang Province, China, it was dried and crushed, ground into powder, and then passed through an 80 mesh sample sieve. Portland cement with grade PO·425 (PO means ordinary Portland cement, it is named according to the Chinese standard ***GB/T 4131-2014 Definition and Terminology of Cement*** [23]), quick lime of 64.4% active CaO content, were used. Second-grade fly ash (according to the Chinese standard ***GB/T 1596-2017 Fly ash used for cement and concrete*** [24] was used after 0.045 mm sieve with the fly ash of the sieve residual less than or equal to 20% is the Chinese standard secondary fly ash). The results of chemical composition analysis of dredged river sediment, cement and fly ash are shown in Table 1. The main component of gypsum is $CaSO_4 \cdot 2H_2O$, which was found to be more than 99%. Aluminum powder is taken from a brick factory named Yushanhong in Songjiang District of Shanghai. A mixer with 0–1100 rpm rotating speed, the lubricating oil and the antifreeze agent were added (There are no specific requirements for lubricating oil and antifreeze agent).

Table 1: Chemical composition of the raw material

Raw material	SiO_2	Al_2O_3	Fe_2O_3	CaO	MgO	Na_2O	K_2O	SO_3	LOI
Dredged river sediment	56.93	18.98	12.05	2.14	2.07	0.70	4.07	0.88	4.13
Cement	22.60	4.63	2.75	65.2	0.78	0.11	0.56	1.84	0.84
Fly ash	53.70	27.30	5.70	7.70	1.80	0.70	0.12	1.60	0.40

Note: Mass fraction (w%, dry basis).

2.2 The Preparation Method of Aerated Concrete Block

The preparation process of the aerated concrete block is shown in Fig. 1. Firstly, the pretreated dredged river sediment, cement, quicklime, fly ash and gypsum were weighed in proportion. Secondly, stir the prepared dry materials by hand. After all the dry materials were mixed, add an appropriate amount of aluminum powder, adjust the water to material ratio to 0.50, and use a mixer for wet mixing for 2–3 min. To improve the characteristics of the slurry, add the antifreeze agent into the slurry, and then

conduct wet mixing for 1 min again. After completely mixing, the slurry was poured into the mold of 100 mm × 100 mm × 100 mm for casting (before pouring the slurry into the mold, the inner wall of the mold was coated with lubricating oil, which helped the subsequent demoulding operation). Then put the poured mold into the blast drying oven to dry, and the temperature was adjusted to 60°C. After 3 h, the power was turned off and waited until the temperature in the oven dropped to room temperature before demoulding (ensure the raised part of the block was cut due to gas generation before demoulding). Then the non-AAC block was placed in the natural environment for natural curing, and after 28 days, the final non-AAC sample was obtained. Then the non-AAC block was placed in the natural environment for natural curing, and after 28 days, the final non-AAC sample was obtained. Then the AAC block was required for the last step by putting the block into autoclave for autoclave curing (autoclave pressure is 2.2 MPa, autoclave temperature is 216°C and autoclave time is 6 h). When the autoclave curing was completed and the temperature in the autoclave reduced to room temperature, the block was put into the blast drying oven again and dried to constant weight at 105°C. The final AAC sample finished [18,25]. The physical drawing of the AAC block is as follows Fig. 2.

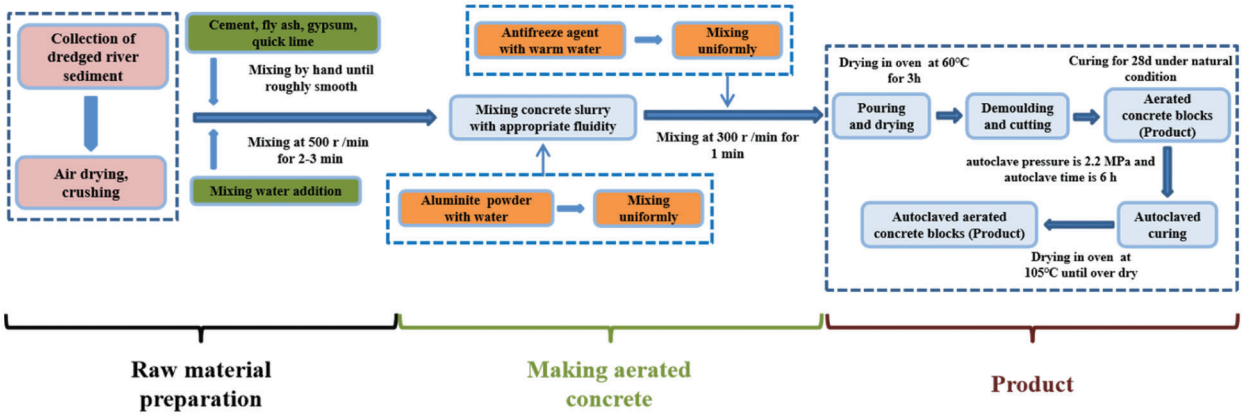

Figure 1: Preparation process of AAC block

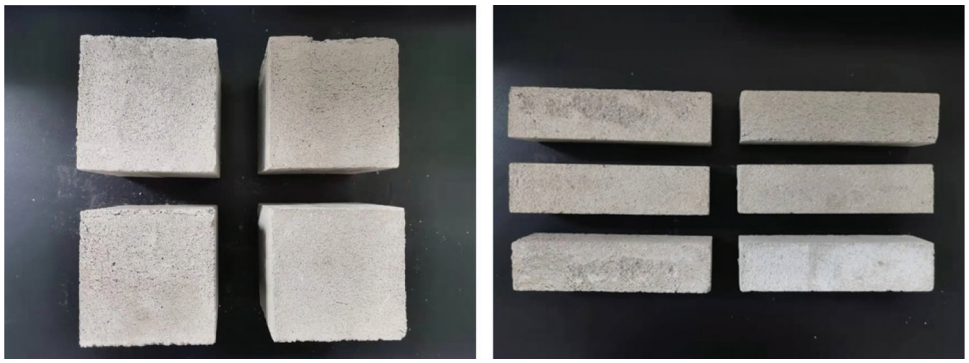

Figure 2: Physical drawing of AAC block

2.3 Characterization Analysis Methods and Instruments

According to ***GB/T 11968-2006 autoclaved aerated concrete blocks*** and ***GB/T 11969-2008 test methods of autoclaved aerated concrete*** [17,26], the size, dry density, compressive strength, water absorption and frost resistance of AAC blocks were tested; The chemical composition of raw materials

was analyzed by X-ray fluorescence spectrometry (version: shimadzuXRF-1800). Field emission scanning electron microscope (SEM) (version: Zeiss Gemini 300) and X-ray diffraction (XRD) (version: Bruker D8 ADVANCE) were used to observe, detect and analyze the microstructure and phase composition of AAC blocks. ICP. MS inductively coupled plasma mass spectrometry (version: NexION 2000B) was determined the content of heavy metals in the block leaching solution.

2.4 Compressive Strength Test Method

The compressive strength of block was tested according to ***GB/T 11969-2008 test method of autoclaved aerated concrete*** [5]. First step, check the appearance of the test piece, especially whether the eight corners are damaged. Second step, measure the size of the test piece to the nearest 1 mm, and calculate the compression area (A) of the test piece. Third step, place the test piece in the center of the lower pressing plate of the material testing machine, and the compression direction of the test piece shall be perpendicular to the expansion direction of the product. Finally, start the testing machine, and when the upper pressing plate is close to the test piece, adjust the ball seat to make the contact balanced. load continuously and evenly at the speed of (2.0 ± 0.5) kN/s until the test piece is damaged, and record the failure load (p). According to ***GB/T 11968-2006 autoclaved aerated concrete blocks*** [6], we expect to reach the compressive strength standard of A5.0 [6]. The calculation formula of blocks' compressive strength was as follows:

$$f = \frac{p}{A} \tag{1}$$

In the formula:

f —— Compressive strength of test piece, MPa.

p —— Failure load, N.

A —— Compression area of test piece, mm^2.

2.5 Dry Density Test Method

The dry density of block was tested according to ***GB/T 11969-2008 test method of autoclaved aerated concrete*** [5]. First step, take a group of three test pieces, measure the axis dimensions in the three directions of length, width and height one by one, accurate to 1 mm, calculate the volume (V) of the test piece, and weigh the mass (M) of the test piece, accurate to 1g. Second step, put the test pieces into the electric blast drying oven, keep it at (60 ± 5)°C for 24 h, then keep it at (80 ± 5)°C for 24 h, final bake it to constant mass (M_0) at (105 ± 5)°C (Constant mass refers to that the mass difference between the two times does not exceed the mass of the test piece every 4 hours during the drying process). According to ***GB/T 11968-2006 autoclaved aerated concrete blocks*** [6], we expect to reach the dry density standard of B07 [6]. The calculation formula of blocks' dry density was as follows:

$$r_0 = \frac{M_0}{V} \times 10^6 \tag{2}$$

In the formula:

r_0 —— Dry density, kg/m^3.

M_0 —— Weight of test piece after drying, in gram, g.

V —— Volume of test piece, mm^3.

2.6 Water Absorption Test Method

Based on the best formulation of AAC (cement 24%, lime 10%, fly ash 34%, dredged river sediment 30% , gypsum 2%, aluminum powder 0.09% and with 0.5 water material ratio), the moisture content of AAC block was studied. Changing the amount of aluminum powder added to the block, six groups of 0%, 0.03%, 0.06%, 0.09%, 0.12%, 0.15% was set up. The moisture content of the block was tested according to ***GB/T 11969-2008 test method of autoclaved aerated concrete*** [26]. First, all the blocks were put in a thermostat water bath with a set constant temperature of (20 ± 5)°C. Under constant temperature, each block was weighed every 12 min in the first 2 h, and then it was weighed again in the 5th h, 10th hour and 20th h, respectively. Finally, each block was weighed every 24 h until the weight of the block was less than 0.1% difference. The calculation formula of block moisture content was as follows:

$$W_S = \frac{M - M_0}{M_0} \times 100\% \tag{3}$$

In the formula:

W_S —— The moisture content, %.

M_0 —— Weight of test piece after drying, in gram, g.

M —— Weight of test piece before drying, in gram, g.

2.7 Frost Resistance Test Method

Based on the best formulation of AAC (cement 24%, lime 10%, fly ash 34%, dredged river sediment 30% , gypsum 2%, aluminum powder 0.09% and with 0.5 water material ratio), the frost resistance of AAC block was studied. After the blocks were made, selected 6 blocks with antifreeze agents and 6 blocks without antifreeze agents respectively [27]. According to ***GB/T 11969-2008 test method of autoclaved aerated concrete*** [26], the frost resistance of the AAC block was tested. The first step was to place the block at (60 ± 5)°C for 24 h, and then at (80 ± 5)°C kept the temperature in the blast drying oven for 24 h, and then dried it to constant weight in the blast drying oven at 105°C. The second step was to immerse the block in a constant temperature water tank, the water surface should be more than 30 mm higher than the block, and the water temperature should be controlled at (20 ± 5)°C. After soaking for 48 h, wiped off the water from the block surface with a wet rag, weighed it and put it into the freezer. The third step was to store it in a freezer at (–20 ± 2)°C for 6 h, then took it out, weighed it and put it into a constant temperature water tank at (20 ± 5)°C for 5 h. The above 11 h operation was a freeze-thaw cycle, and the freeze-thaw cycle was repeated more than 15 times. Recorded the damage of the block every 5 times. If the block was damaged seriously, took out the test block to stop the freeze-thaw experiment, and recorded the number of freeze-thaw cycles. Finally, after 15 times freeze-thaw cycles, put it into the blast drying oven, and dried the block to constant weight according to the first step. After the freeze-thaw cycle, measure the weight of the block according to the steps in 2.5. Then measure the compressive strength of the block according to the steps in 2.4.

3 Results and Discussion

3.1 Influence of Fly Ash and Dredged River Sediment on Physical and Mechanical Performances of Aerated Blocks

The dredged river sediment not only has the characteristics of strong binding and high plasticity, but also has the content of SiO_2 as high as 41%, which can provide a large amount of Si element for the preparation of aerated concrete blocks with improved compressive strength. The influence of the dredged river sediment and fly ash mix ratio on dry density and compressive strength of aerated concrete blocks is the key performance indicator. The formulation of aerated concrete block is based on the previous exploratory

experiment: the cement lime ratio of 2.4:1 is adopted and prepared in two dosage ratios. Formulation A is 24% cement and 10% lime. Formulation B adopts 48% cement and 20% lime. The two formulations both with 2% gypsum, 0.09% aluminum powder added and with 0.5 water material ratio, then the Formulation A with 64% added dredged river sediment and fly ash, while the Formulation B remains at 30%. Both Formulations A and B are used to make AAC blocks and non-AAC blocks with the pressure, temperature and duration of curing (2.2 MPa, 216°C and 6 h) remained unchanged.

Due to the fixed amount of cement, lime and gypsum, the content of dredged river sediment and fly ash in formulations A and B are 64% and 30%, respectively. For recycling resources, it is necessary to ensure to maximize the utilization of dredged river sediment. When the cement content is 24% and the fly ash content is less than 20%, the compressive strength of the AAC block is 3.4 MPa, which is lower than the standard requirements of A 5.0 (The standard A 5.0 according to ***GB/T 11968-2006 autoclaved aerated concrete block*** [17]). When the cement content is 48% and the fly ash content is less than 10%, the compressive strength of non-AAC concrete block is 2.35 MPa and the dry density is 910.21 kg/m³, these two indicators do not meet the standards of C 3 and A 09. Therefore, the dredged river sediment content of Formulation A should be controlled between 22%–42%, and the Formulation B is 11%–21%, in the hope to reach the AAC block standards of B 07 and A 5.0 or non-AAC block standards of A 09 and C 3. At the same time, the difference between AAC block and non-AAC block prepared with the same formulation can be compared. The formulation of the aerated concrete block is shown in Tables 2 and 3.

Table 2: Changing dredged river sediment and fly ash content on aerated concrete blocks with 24% cement content

No.	Cement	Lime	Fly ash	Dredged river sediment	Gypsum	Aluminum power	Water material ratio
1	24	10	42	22	2	0.09	0.5
2	24	10	38	26	2	0.09	0.5
3	24	10	34	30	2	0.09	0.5
4	24	10	32	32	2	0.09	0.5
5	24	10	30	34	2	0.09	0.5
6	24	10	26	38	2	0.09	0.5
7	24	10	22	42	2	0.09	0.5

Note: Mass fraction (w%, dry basis).

Table 3: Various dredged river sediment and fly ash contents on aerated concrete blocks with 48% cement content

No.	Cement	Lime	Fly ash	Dredged river sediment	Gypsum	Aluminum power	Water material ratio
1	48	20	19	11	2	0.09	0.5
2	48	20	17	13	2	0.09	0.5
3	48	20	15	15	2	0.09	0.5
4	48	20	13	17	2	0.09	0.5
5	48	20	11	19	2	0.09	0.5
6	48	20	9	21	2	0.09	0.5

Note: Mass fraction (w%, dry basis).

Figs. 3 and 4 show the influence of the different proportions of dredged river sediment and fly ash on aerated concrete blocks. Fig. 3 is based on the experimental data obtained from Formulation A, while Fig. 4 is based on Formulation B. Fig. 3a is the nonlinear fitting curve representation of dry density and compressive strength of AAC block, Fig. 3b is the comparison of dry density and compressive strength between AAC block and non-AAC block and Fig. 3c is the comparison of dry density and compressive strength of non-AAC block at 7 d, 14 d and 28 d. Fig. 3a shows that the compressive strength of the AAC block is the best with the dredged river sediment in the range of 30%–34%, and the dry density is within 725 kg/m^3. When the content of the dredged river sediment is 30%, the dry density of the AAC block is 716.56 kg/m^3. At the same time, the compressive strength is at peak value, and its average compressive strength is about 4.5 MPa. The dry density and compressive strength both meet the standards of B 07 and A 5.0 in ***GB/T 11968-2006 autoclaved aerated concrete blocks*** [17]. Then with regression analysis, the correlation between dry density and compressive strength of AAC block can be established, and the relationship between the amount of dredged river sediment and the dry density and compressive strength of the block is obtained using the equation as follows.

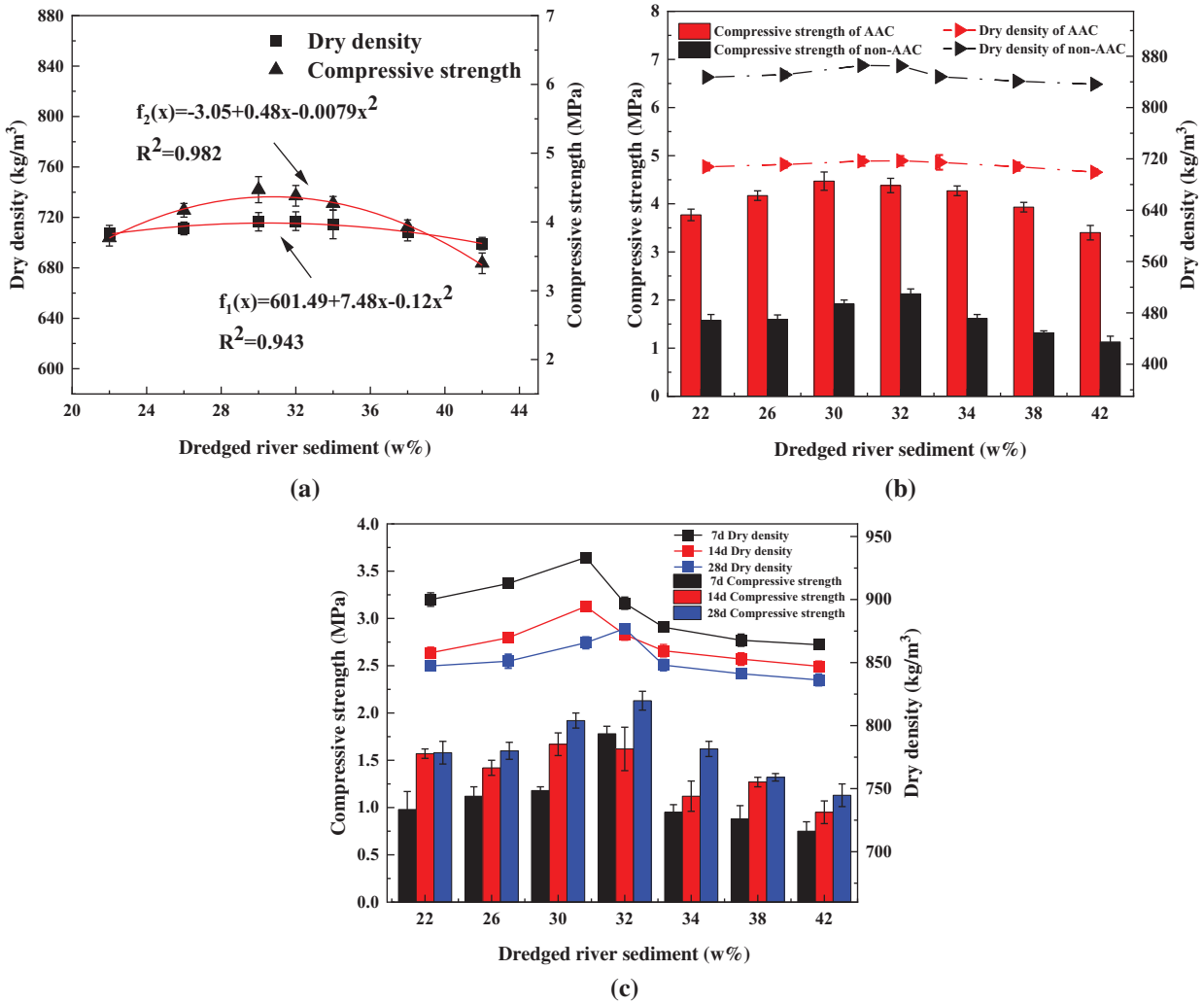

Figure 3: Comparison of dry density and compressive strength of autoclaved and non-AAC blocks with 24% cement content

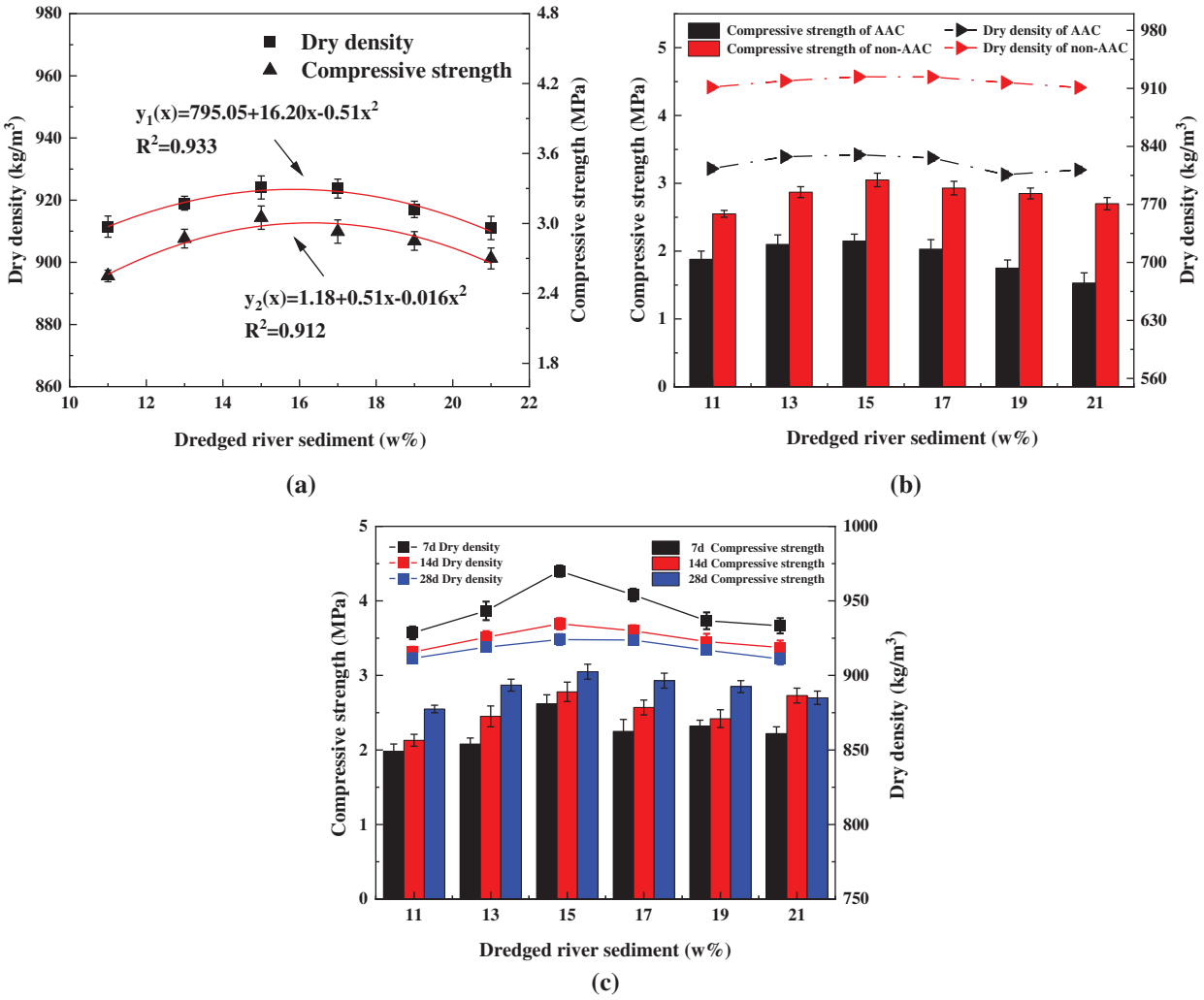

Figure 4: Comparison of dry density and compressive strength of autoclaved and non-AAC blocks with 48% cement content

$$f_1(x) = 601.49 + 7.48x - 0.12x^2 (R^2 = 0.943) \tag{4}$$

In the formula:

$f_1(x)$ —— dry density, kg/m^3

x —— proportion of dredged river sediment, %,

$$f_2(x) = -3.05 + 0.48x - 0.0079x^2 (R^2 = 0.982) \tag{5}$$

In the formula:

$f_2(x)$ —— compressive strength, MPa.

x —— proportion of dredged river sediment, %.

The regression Eqs. (4) and (5) are in good agreement with the experimental data, indicating that there is a correlation between the dredged river sediment content, dry density and also the compressive strength of the AAC block. The nonlinear fitting curve is shown in Fig. 3a. The property of non-AAC block using this

formula is not ideal, and the measured values of dry density and compressive strength did not reach the standard C 3 of ***JG/T 266-2011 foam concrete*** [28]. This can be explained as, firstly steam cured concrete can greatly reduce the original density of concrete blocks and secondly, under the condition of high temperature and pressure, the hydration process is accelerated and the extent of the hydration reaction is more than under non-autoclaved conditions. As a result, the crystallinity of hydrated calcium silicate has been increased, and the amount of CSH and tobermorite are also increased, finally, compressive strength improved. At the same time, fly ash can improve the early and late compressive strength of the concrete slurry during the curing process [29–31]. In the meantime, it is speculated that the reason why the compressive strength of non-AAC block does not meet the standard, could be related to the reduced cement content which is the main provider of Ca. In the case of maintaining the natural condition, the hydration reaction is not completed, the utilization rate of Ca in cement is low, and a majority of CSH and tobermorite cannot be formed, so the compressive strength is expected to be low. Therefore, by considering all the factors, the best formulation is cement 24%, lime 10%, fly ash 30%–34%, dredged river sediment 30%–34%, gypsum 2%, aluminum powder 0.09% and with 0.5 water material ratio. It can be seen that it is better to prepare the AAC block with Formulation A.

Fig. 4a shows that the 6 formulations all achieve the standards of A 09 and C 3 in ***JG/T266-2011 foam concrete*** [28]. When the dredged river sediment content is 15%, the best compressive strength of non-AAC has been achieved [28]. The correlation amongst the dry density, compressive strength of the non-AAC block, and the relationship between the amount of dredged river sediment showed good correlation and the equation of dry density or compressive strength of the block is obtained as follows:

$$y_1(x) = 795.05 + 16.20x - 0.51x^2 (R^2 = 0.933) \tag{6}$$

In the formula:

$y_1(x)$ —— dry density, kg/m^3.

x —— proportion of dredged river sediment, %.

$$y_2(x) = 1.18 + 0.51x - 0.016x^2 (R^2 = 0.912) \tag{7}$$

In the formula:

$y_2(x)$ —— compressive strength, MPa.

x —— proportion of dredged river sediment, %.

The regression Eqs. (6) and (7) are in good agreement with the experimental data, indicating that there are correlations between sediment content with dry density and compressive strength of non-AAC blocks. The nonlinear fitting curve is shown in Fig. 4a. The performance of the AAC block with this formulation is not ideal, the measured values of dry density and compressive strength did not meet the standard of ***GB/T 11968-2006 autoclaved aerated concrete blocks*** [17]. The reason for the result in Fig. 4 is that the increase of cement content provides a large amount of Ca element, so that the Si element in fly ash and dredged river sediment can be fully utilized, resulting in more CSH and tobermorite were formed, so the compressive strength value is reasonable [29,30]. However, tobermorite has an adsorption effect on Cr^{3+}. At the same time, the adsorption of Cr^{3+} leads to the precipitation of structural Ca^{2+} in the tobermorite channel, resulting in damage to crystallinity [32]. For the comprehensive consideration, the best formulation is 48% cement, 20% lime, 15% fly ash, 15% dredged river sediment, 2% gypsum, 0.09% aluminum powder and 0.5 water material ratio to prepare non-AAC block. It can be seen that it would be better to prepare non-AAC block with Formulation B.

Therefore, when the close content of dredged river sediment and fly ash has been used, the quality of AAC block or non-AAC block is the best. On the premise of maximizing the use of dredged river

sediment and reducing the consumption of raw materials, Formulation A is the most suitable for preparing AAC blocks. When steam curing equipment is not available, Formulation B can also be used to prepare the non-AAC blocks.

3.2 Effect of Aluminum Powder Addition on the Moisture Content of AAC Block

Fig. 5a shows that the moisture content of concrete blocks in six groups with different aluminum powder content during 0–2 h. Fig. 5b shows that the moisture content of concrete blocks in six groups with different aluminum powder content during 5–120 h. Overall, in a certain range, the higher the aluminum powder, the higher the moisture content. The moisture content of the block in the first 2 hours changes quite rapidly, and the moisture content of the block increases at a higher rate in the first 0.2 hours. The moisture content of all the blocks reaches more than half of the final moisture content in the first 0.2 hours. In the later time, with the extension of immersion time, the increase of moisture content gradually plateaued.

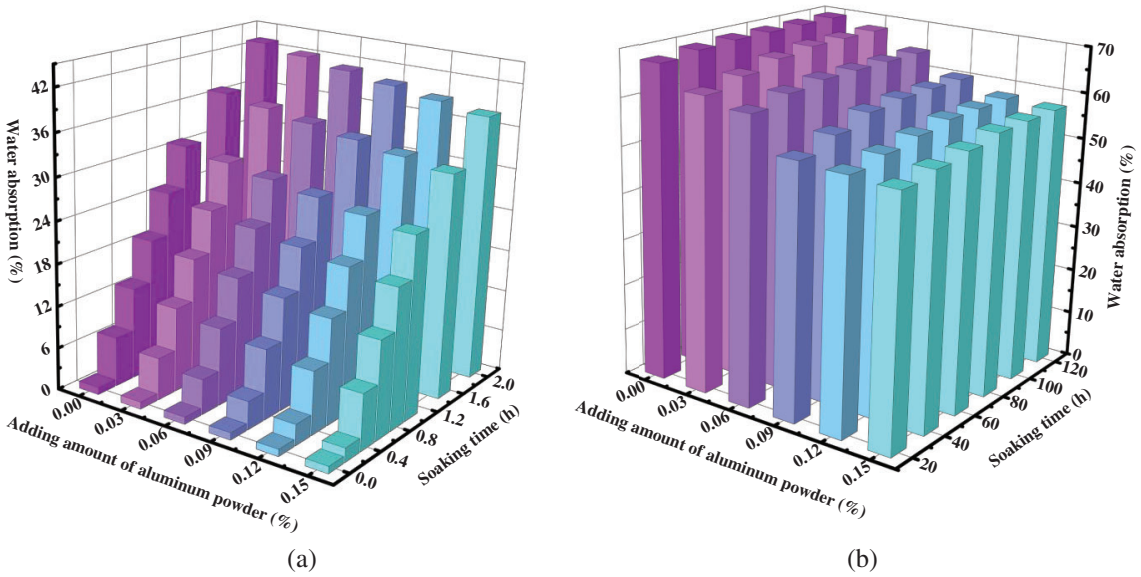

Figure 5: Variation of moisture content in 0–120 h with different aluminum powder dosage

The reason is that the block contains large amount of substances in which are easy to absorb water, such as dredged river sediment and fly ash. In the first two hours, the moisture content of the block increased rapidly because the water absorbed by the block was in the form of gap water. The different aluminum powder added to the block resulted in different porosity and pore size of the block, and also affected the moisture content of the block. With the development with the immersion time, the water in the block changes from gap water to capillary water and surface adsorption water. Capillary water and adsorbed water formed slowly, and is difficult to be removed [33].

3.3 The Influence of Moisture Content of AAC Block on Its Compressive Strength

Based on the best formulation (cement 24%, lime 10%, fly ash 34%, dredged river sediment 30%, gypsum 2%, aluminum powder 0.09% and with 0.5 water material ratio), the test results of the moisture content can be divided into eight groups (0%, 5%, 10%, 20%, 30%, 40%, 50%, 60%) to test the compressive strength under different moisture content. According to the test procedures, the basic moisture content of all blocks reaches saturation after 60 h. All blocks with saturation moisture were put into the blast drying oven with the temperature set at (60 ± 5)°C. Each sample was dried to the required

moisture content after different waiting times. The influence of moisture content on the compressive strength of the AAC block is shown in Fig. 6.

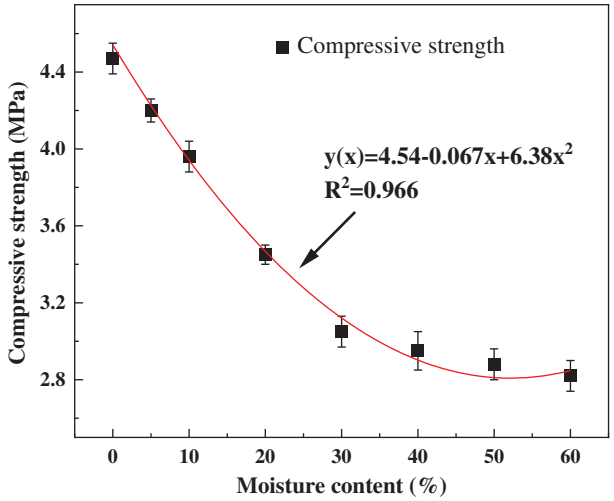

Figure 6: Relationship between moisture content and compressive strength of AAC blocks

Fig. 6 is the direct data comparison of the influence of the AAC block's moisture content on its compressive strength. It can be seen from Fig. 6 that with the increase of the block's moisture content, the compressive strength of the block gradually decreases. Fig. 6 shows that the linear relationship between the moisture content of blocks and the compressive strength of blocks. The moisture content increases and the compressive strength of the block reduce. The moisture content is between 0%–30%, especially in 0%–10%, the compressive strength of the block decreases most. Then the moisture content of the block is between 30%–60%, the compressive strength of the block changes slowly.

$$y(x) = 4.54 - 0.067x + 6.38x^2 (R^2 = 0.966) \tag{8}$$

In the formula:

$y(x)$ —— compressive strength, MPa.

x —— moisture content, %.

The regression Eq. (8) is in good agreement with the experimental data, which indicates that there is a nonlinear fitting curve correlation between the moisture content and the compressive strength of blocks. The nonlinear fitting curve is shown in Fig. 6. Fig. 6 shows that when the moisture content is between 10% and 30% during the first stage, the AAC block absorbs a large portion of water, causing the internal pores of the block to be filled with free water. Therefore, the particle bonding force between the internal pores is weakened, and the internal structure changes suddenly, resulting in a significant reduction in its compressive strength [33]. When the moisture content of the AAC block exceeds 30%, the changing trend of compressive strength of the block slows down. The reason may be that the free water in its internal pores is saturated, and the moisture content continues to increase in the form of adsorbed water, while the change of internal structure of the block is not obvious, therefore, the compressive strength changes little and tends to be stable when the moisture content exceeds 30%.

3.4 Frost Resistance of AAC Block

The frost resistance of the AAC block is shown in Tables 4 and 6, Fig. 7. Table 4 shows the effect of frozen-thaw action on the weight of the AAC blocks without antifreeze added. It can be seen from Table 4 that with the increase of freeze-thaw cycles, the weight of the block increases, but after the fifth time freeze-thaw cycle, the weight of the block is greatly reduced. The reason may be that the surface of the block suffers from a large area of erosion and falls off, the appearance is seriously damaged, and the experiment is stopped.

Table 4: Effect of freeze-thaw action on the weight of AAC blocks without antifreeze added

Freeze thaw cycles	Weight of block 1(g)	Weight of block 2(g)	Weight of block 3(g)	Weight of block 4(g)	Weight of block 5(g)	Weight of block 6(g)
0	246.2	244.7	242.8	245.0	245.3	243.1
1	408.4	405.3	407.7	409.2	408.9	403.3
2	408.9	406.1	408.3	410.1	409.3	403.9
3	409.9	406.4	409.0	409.7	409.7	404.1
4	361.7	406.9	405.1	407.1	406.2	399.7
5	—	392.4	379.4	398.8	401.1	352.9
6	—	377.9	—	362.9	382.8	—
7	—	—	—	—	—	—

Note: "—": Represents that the block is seriously damaged and cannot be weighed.

Table 6 shows the data of compressive strength test of AAC block with antifreeze agent after 15 times frozen-thaw cycles. After 15 times frozen-thaw, the average strength of AAC block is 3.1 MPa, and the loss rate of compressive strength is 31.11%.

Fig. 7 is the curve relationship between the weight of AAC block with antifreeze agent and the number of freeze-thaw cycles. Through the effect of freeze-thaw, at first, the weight of the block increases and then decreases. After 15 times freeze-thaw cycles, the block still has no obvious damage traces, and the mass loss rate of a block is less than 5%. After that, a regression equation is obtained based on the relationship between weight and freeze-thaw cycles of AAC blocks, which is shown as the following:

$$\mathrm{F}(x) = 381.99 + \frac{255.36}{13.73 \times \sqrt{\frac{\pi}{2}}} e^{-2\frac{(x-8.09)^2}{13.73^2}} \quad (R^2 = 0.941) \tag{9}$$

In the formula:

$\mathrm{F}(x)$ —— compressive strength, MPa.

x —— moisture content, %.

The regression Eq. (9) is in good agreement with the experimental data, which indicates that there is a nonlinear fitting curve correlation between the number of freeze-thaw cycles and the weight of the AAC block. The nonlinear fitting curve is shown in Fig. 7. Table 5 shows the compressive strength data of AAC blocks with antifreeze before freezing and thawing. As is shown in Fig. 7, in the early stage of the freeze-thaw cycle, the quality of blocks increases, because the hydration reaction inside the block combined with free water forms silica gel, which leads to the increase of the weight of the block [27,34–37]. Then the freeze-thaw erosion intensifies, and the block surface has spalling or cracks, so in

the second half of the freeze-thaw experiments, the block mass slowly decreases. To sum up, based on the best formulation of AAC (cement 24%, lime 10%, fly ash 34%, dredged river sediment 30%, gypsum 2%, aluminum powder 0.09% and with 0.5 water material ratio), the frost resistance of the AAC block is poor without antifreeze, so it cannot be used in alpine areas. After adding antifreeze, the antifreeze effect of the block is significantly improved, and after 15 standard freeze-thaw cycles, the compressive strength of the block can still meet more than 3 MPa (A3.5).

Table 5: Compressive strength of AAC blocks before freeze-thaw

No.	Compressive strength/MPa
1	4.4
2	4.5
3	4.4
4	4.5
5	4.5
6	4.5

Table 6: Compressive strength of AAC blocks after 15 freeze-thaw cycles

No.	Compressive strength/MPa
1	3.0
2	3.1
3	3.0
4	3.1
5	3.2
6	3.1

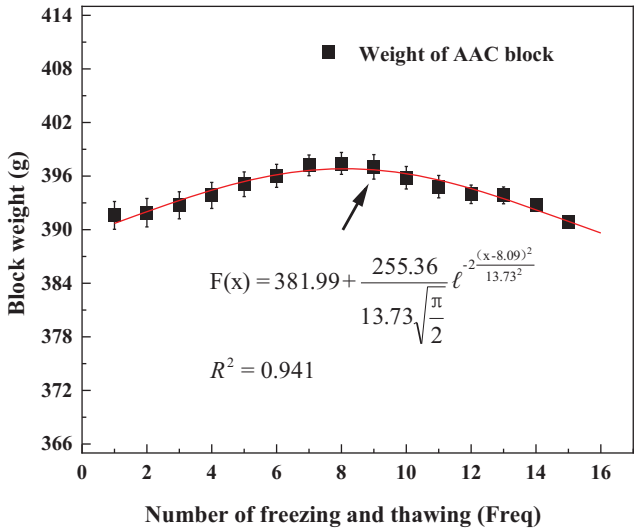

Figure 7: Relationship between the weight of AAC blocks and the number of freeze-thaw cycles

3.5 Precipitation Analysis of Heavy Metals

Due to the accelerated process of contemporary urbanization, the amount of production and domestic sewage increases, and domestic sewage and industrial and agricultural wastewater are discharged into the river. These pollutants are transformed into solid phase through physical and chemical action and then deposited in the dredged river sediment, resulting in excessive heavy metals in the dredged river sediment. Therefore, it is necessary to detect whether the heavy metal content of AAC blocks prepared from dredged river sediment exceeds the standard. Several AAC blocks were prepared based on the best formulation (cement 24%, lime 10%, fly ash 34%, dredged river sediment 30%, gypsum 2%, aluminum powder 0.09% and with 0.5 water material ratio). According to ***HJ 557-2010 Solid Waste-Extraction procedure for leaching toxicity-Horizontal vibration method*** and ***SL 394.2-2007 Determination of 34 elements (Pb, Cd, V, P, etc.). Inductively coupled plasma mass spectroscopy (ICP-MS)*****,** determines whether the heavy metal content of the block exceeds the standard [38,39]. Seven heavy metal elements, Cd, Cr, Cu, Pb, Mn, Zn and As, were selected for metal analysis. In the solid waste leaching solution, except Cr, the content of the other six heavy metal elements was below the detection limit, while the average content of Cr was 4.23 ug/L. Table 7 shows the contents of the above seven heavy metals in the block leaching solution. In addition, the sample will not dissolve for a longer period of time. Because when the experiment of precipitating analysis of heavy metals, we adopted the method of multiple sampling and detection in multiple periods. The data in Table 7 is the content of heavy metal ions in the leaching solution measured after the blocks were immersed for 24 h. Before that, we measured the content of heavy metal ions in the leaching solution after 12 h and 18 h, respectively, and the measured data in the three periods were within 0.1%. It indicates that AAC block can fix heavy metal elements well, and will not harm the environment and human beings when it is used in production and life.

Table 7: Contents of seven heavy metals in the block leaching solution

Detected heavy metals element	Detection results (ug/L)	Detection limit (ug/L)	Lower limit of determination (ug/L)
Cd	ND	1.2	4.8
Cr	4.23	2.0	8.0
Cu	ND	2.5	10.0
Pb	ND	4.2	17.0
Mn	ND	3.6	14.4
Zn	ND	6.4	25.6
As	ND	1.0	4.0

Note: 1. “ND” means not detected.

3.6 SEM Analysis

SEM morphology of AAC block prepared by mixing a certain amount of fly ash and dredged river sediment in different proportions is shown in Fig. 8. It can be seen from Fig. 8 that a large number of micropores are distributed inside the block, which is the main reason for the low dry density of the block. However, there are a lot of crystallites around the pores. According to the phase analysis of XRD, the main contents in the block are tobermorite (needle or sheet), SiO_2 and C-S-H. After 10000 times magnifications, it can be seen that the needle like hydration product, tobermorite and C-S-H interweave with each other to form a network skeleton, which is the main reason for the block to have a certain compressive strength [40]. It can be seen from the two magnifications, 4000 and 10,000 times, topographic maps, when the proportion of dredged river sediment and fly ash are different, the needle

hydration product tobermorite of the block is fine. However, when the proportion of dredged river sediment and fly ash are close, the needle hydrated tobermorite of the block is thicker [37]. And from the high-power microscope, it can be perceived that, in contrast, the skeleton hierarchical structure of blocks with a similar proportion of dredged river sediment and fly ash is more compact. Therefore, in the above water content and frost resistance tests, under the action of etching and freeze-thaw erosion respectively, the thicker needle hydration products are more resistant to erosion, so as to ensure that the compressive strength of the block is not weakened.

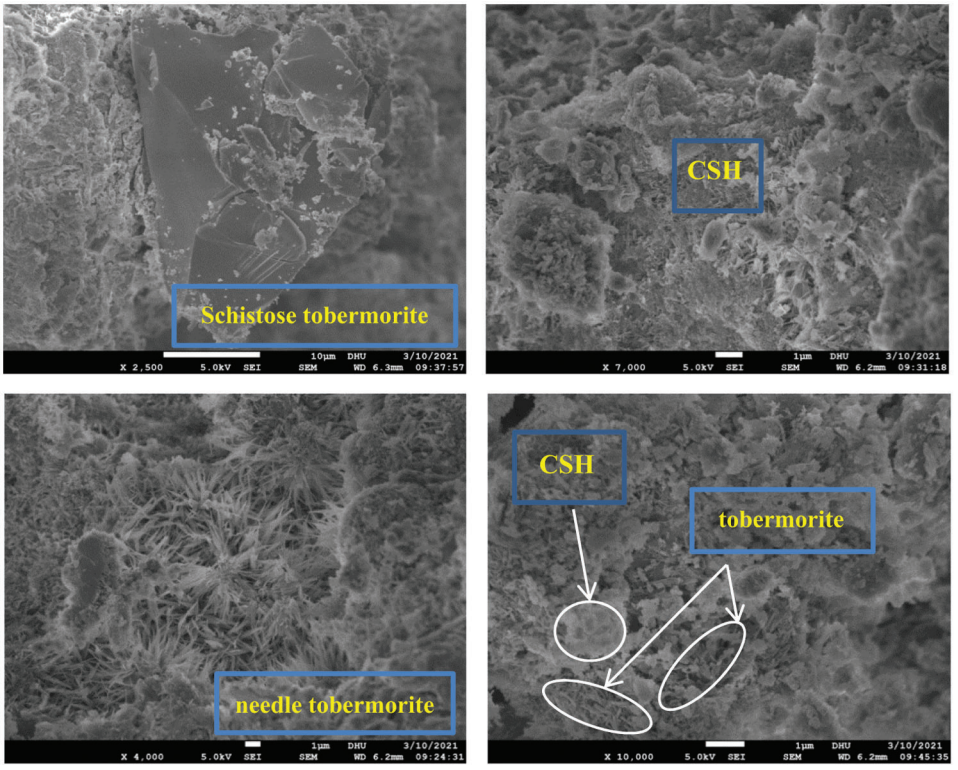

Figure 8: SEM spectrum of AAC blocks with different dredged river sediment content

3.7 XRD Analysis

The XRD patterns of AAC block samples with different proportions of dredged river sediment and fly ash are shown in Fig. 9. A large number of dispersion peaks of CSH and diffraction peaks of tobermorite can be seen from the XRD patterns. Under the condition of the 2.2 MPa autoclaved pressure and the 6 h autoclave time, the hydrated tobermorite. The chemical equation of tobermorite formation is shown in Eq. (10), it is formed by the reaction of calcium hydroxide and quartz in the block. The main products have the characteristics of needle and sheet shape, with small density, lightweight and high strength. In addition, there is a large number of unreactive quartz particles are present, therefore, CSH gel plays a major role in cementing. It can be observed from Fig. 9 that the diffraction peak of tobermorite shows a trend of first strengthening and then weakening with the increase of channel sediment [41]. It is also proved that the amount of dredged river sediment is between 30% and 34%, and the compressive strength of the block is the best. XRD results also show that the main components of AAC block are Quartz (SiO_2), Calcium Hydroxyl Silicate ($Ca_9(Si_6O_{18}H_2)\cdot 2H_2O$) and Cebollite ($Ca_5Al_2(OH)_4Si_3O_{12}$). It can be seen that a large amount of Ca^{2+} is released by cement reaction, while a large amount of SiO_2 is contained in fly ash and dredged river sediment, and a large amount of hydrated calcium silicate is generated by the reaction of fly ash and dredged river sediment. This kind of material has a large specific surface area, strong surface activity, light texture, grayish white and is easy to agglomerate, so it can connect well with minerals, especially tobermorite and aluminum substituted tobermorite, it can increase the strength of the block.

$$CaO + H_2O == Ca(OH)_2 + SiO_2 \rightarrow C-S-H \rightarrow C_5S_6H_5 \tag{10}$$

$$xCa(OH)_2 + SiO_2 + nH_2O \rightarrow xCaO \cdot SiO_2 \cdot mH_2O$$

$$xCa(OH)_2 + SiO_2 + nH_2O + Al_2O_3 \rightarrow xCaO \cdot SiO_2 \cdot mH_2O + Ca(OH)_2 \cdot Al_2O_3 \cdot \ SiO_2 \cdot H_2O$$

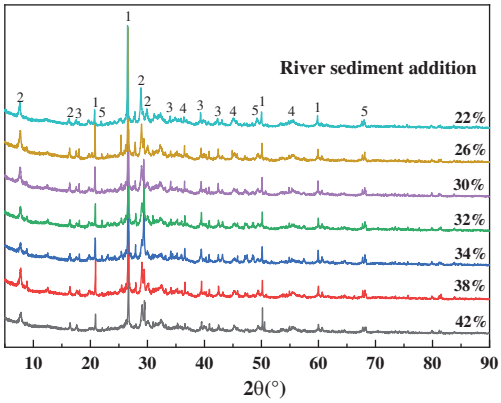

1: Quartz (SiO_2) 2: Alminum tobermorite ($Ca_5Si_5Al(OH)O_{17}\cdot 5H_2O$)
3: Calcium Silicate Hydrate (C-S-H) 4: Cebollite ($Ca_5Al_2(OH)_4Si_3O_{12}$)
5: Calcium Hydrogen Silicate Hydroxide Hydrate ($Ca_9(Si_6O_{18}H_2)(OH)_{18}\cdot 2H_2O$)

Figure 9: XRD pattern of AAC blocks with different dredged river sediment content

4 Conclusion

It is feasible to use the dredged river sediment as the main raw material for the preparation of aerated concrete blocks. The average dry density and compressive strength of AAC block were 716.56 kg/m³ and 4.5 MPa, respectively, under the conditions of 30%–34% dredged river sediment, 24% cement, 10% lime, 30% fly ash, 2% gypsum 0.09% aluminum powder and the 0.5 water to material ratio, with 2.2 MPa of autoclaved pressure and 6 h of autoclaved time. Its performance index meets the requirements of A

5.0 and B 07 in ***GB/T 11968-2006 autoclaved aerated concrete block*** [17]. Moreover, under the conditions of 15% dredged river sediment, 48% cement, 20% lime, 15% fly ash, 2% gypsum, 0.09% aluminum powder and the 0.5 water to material ratio, also can get the non-AAC block, which reaches the standard of ***JG/T 266-2011 foam concrete*** [28].

AAC block has a strong water absorption ability, and high moisture content has a great impact on the compressive strength of the block. When the moisture content of the block is within 30%, the numerical value of its compressive strength decreases rapidly. After the moisture content of the block is 30%, the change of compressive strength tends to be stable and maintained at about 3 MPa, which meets the industrial use standard.

When preparing AAC blocks, adding 0.1% cement antifreeze can significantly improve the frost resistance of autoclaved blocks. The compressive strength of blocks after 15 cycles of freeze-thaw can also reach more than 3 MPa, which meets the industrial use standard.

Microstructural analysis shows that the main components of AAC block are tobermorite, quartz, calcium silicate hydrate and CSH gel. A large number of floc like CSH gel cemented a large number of crystals to enhance the compressive strength of blocks. During this period, the chemical bonds between Si-O-Si and Al-O-Al broke, and Al-O-Si was regenerated, resulting in better strength alumina tobermorite, which further improved the compressive strength of AAC blocks. The low density of the block is due to a large number of needle shaped tobermorite interspersed together, forming a unique porous structure of AAC block.

Acknowledgement: This work was supported by the Donghua University and Shanghai Jiaotong University.

Funding Statement: This work was supported by the National Natural Science Foundation of China (NSFC) (Nos. 21876025, 42177119). https://isisn.nsfc.gov.cn/egrantindex/funcindex/prjsearch-list.

Conflicts of Interest: The authors declare that they have no conflicts of interest to report regarding the present study.

References

1. Zhao, J., Wu, E., Bai, X., Lei, P., Gao, Y. (2021). Pollution characteristics and ecological risks associated with heavy metals in the Fuyang river system in North China. *Environmental Pollution, 281(2),* 116994. DOI 10.1016/j.envpol.2021.116994.
2. Kim, I. G., Kim, Y. B., Kim, R. H., Hyon, T. S. (2021). Spatial distribution, origin and contamination assessment of heavy metals in surface sediments from Jangsong tidal flat, Kangryong river estuary, DPR Korea. *Marine Pollution Bulletin, 168(7),* 112414. DOI 10.1016/j.marpolbul.2021.112414.
3. Dendievel, A. M., Mourier, B., Dabrin, A., Delile, H., Coynel, A. et al. (2020). Metal pollution trajectories and mixture risk assessed by combining dated cores and subsurface sediments along a major European river (Rhone River, France). *Environment International, 144(4),* 106032. DOI 10.1016/j.envint.2020.106032.
4. Niu, Y., Jiang, X., Wang, K., Xia, J., Yu, H. (2019). Meta analysis of heavy metal pollution and sources in surface sediments of Lake Taihu. *China Science of the Total Environment, 700(1),* 134509. DOI 10.1016/j.scitotenv.2019.134509.
5. Xie, L., Zhang, Z. (2015). Sources and pollution assessment of heavy metals in the sediment of the tidal flat at the Yuantuojiao piont, the north brand, Changjiang River. *Scientia Geographica Sinica, 35,* 380–386. DOI 10.13249/j.cnki.sgs.2015.03.018.
6. Yang, X. (2020). *Conversion of contaminated dredged river sediment into lightweight construction materials and heavy metal solidification*. (Master Thesis). Shanghai Jiao Tong Universuty, Shanghai.
7. Song, B., Zeng, G., Gong, J., Liang, J., Xu, P. et al. (2017). Evaluation methods for assessing effectiveness of in situ remediation of soil and sediment contaminated with organic pollutants and heavy metals. *Environment International, 105(7),* 43–55. DOI 10.1016/j.envint.2017.05.001.

8. Song, S., Zhao, T. (2019). Study on the present situation and development of river sediment treatment and disposal. *China Resources Comprehensive Utilization, 37,* 28–30. DOI 10.3969/j.issn.1008-9500.2019.09.009.
9. Chao, Z., Shan, B., Zhu, Y., Tang, W. (2018). Remediation effectiveness of Phyllostachys pubescens biochar in reducing the bioavailability and bioaccumulation of metals in sediments. *Environmental Pollution, 242,* 1768–1776. DOI 10.1016/j.envpol.2018.07.091.
10. Mulligan, C. N., Yong, R. N., Gibbs, B. F. (2001). An evaluation of technologies for the heavy metal remediation of dredged sediments. *Journal of Hazardous Materials, 85(1–2),* 145–163. DOI 10.1016/S0304-3894(01)00226-6.
11. Sun, Q., Ding, S., Chen, M., Gao, S., Lu, G. et al. (2019). Long-term effectiveness of sediment dredging on controlling the contamination of arsenic, selenium, and antimony. *Environmental Pollution, 245(3),* 725–734. DOI 10.1016/j.envpol.2018.11.050.
12. Zhang, Y., Labianca, C., Chen, L., de Gisi, S., Notarnicola, M. et al. (2021). Sustainable *ex-situ* remediation of contaminated sediment: A review. *Environmental Pollution, 287(3),* 117333. DOI 10.1016/j.envpol.2021.117333.
13. He, X., Zheng, Z., Yang, J., Su, Y., Wang, T. et al. (2020). Feasibility of incorporating autoclaved aerated concrete waste for cement replacement in sustainable building materials. *Journal of Cleaner Production, 250(4),* 119455. DOI 10.1016/j.jclepro.2019.119455.
14. Jin, Y., Fw, A., Xha, B., Ying, S., Tw, A. et al. (2021). Potential usage of porous autoclaved aerated concrete waste as eco-friendly internal curing agent for shrinkage compensation. *Journal of Cleaner Production, 320(11),* 128894. DOI 10.1016/j.jclepro.2021.128894.
15. Cai, Q., Ma, B., Jiang, J., Wang, J., Shao, Z. et al. (2021). Utilization of waste red gypsum in autoclaved aerated concrete preparation. *Construction and Building Materials, 291,* 123376. DOI 10.1016/j.conbuildmat.2021.123376.
16. Nadeem, Z., Mcyotto, F., Wei, Q. (2020). Utilization of construction and demolition waste, fly ash waste in autoclaved aerated concrete. *Advance in Environmental Waste Management & Recycling, 3,* 1–5. DOI 10.33140/aewmr.03.02.01.
17. Autoclaved Aerated Concrete Blocks (2006). GB 11968-2006 C.F.R.
18. Peng, Y., Liu, Y., Zhan, B., Xu, G. (2021). Preparation of autoclaved aerated concrete by using graphite tailings as an alternative silica source. *Construction and Building Materials, 267(5),* 121792. DOI 10.1016/j.conbuildmat.2020.121792.
19. Wang, L., Shao, Y., Zhao, Z., Chen, S., Shao, X. (2020). Optimized utilization studies of dredging sediment for making water treatment ceramsite based on an extreme vertex design. *Journal of Water Process Engineering, 38,* 101603. DOI 10.1016/j.jwpe.2020.101603.
20. Chen, Y., Shi, J., Rong, H., Zhou, X., Chen, F. et al. (2020). Adsorption mechanism of lead ions on porous ceramsite prepared by co-combustion ash of sewage sludge and biomass. *Science of the Total Environment, 702,* 135017. DOI 10.1016/j.scitotenv.2019.135017.
21. Slimanou, H., Eliche-Quesada, D., Kherbache, S., Bouzidi, N. (2019). Harbor dredged sediment as raw material in fired clay brick production: Characterization and properties. *Journal of Building Engineering, 28(4),* 101085. DOI 10.1016/j.jobe.2019.101085.
22. Yang, X., Zhao, L., Haque, M. A., Chen, B., Ren, Z. et al. (2020). Sustainable conversion of contaminated dredged river sediment into eco-friendly foamed concrete. *Journal of Cleaner Production, 252(2),* 119799. DOI 10.1016/j.jclepro.2019.119799.
23. Nomenclature and Terminology of Cement (2014). GB/T 4131-2014 C.F.R.
24. Fly Ash Used for Cement and Concrete (2017). GB/T 1596-2017 C.F.R.
25. Zhang, H., Xu, K., Chen, Y., Yue, S., Qi, C. et al. (2019). Preparation of autoclaved aerated concrete with construction waste and alkali residue. *Chinese Journal of Environmental Engineering, 13,* 441–448.
26. Test Methods of Autoclaved Aerated Concrete (2020). GB/T 11969-2020 C.F.R.
27. Wang, F., Ping, X., Zhou, J., Kang, T. (2019). Effects of crumb rubber on the frost resistance of cement-soil. *Construction and Building Materials, 223(2),* 120–132. DOI 10.1016/j.conbuildmat.2019.06.208.
28. Foamed Concrete (2011). JG/T 266-2011 C.F.R.

29. Cai, L., Ma, B., Li, X., Lv, Y., Liu, Z. et al. (2016). Mechanical and hydration characteristics of autoclaved aerated concrete (AAC) containing iron-tailings: Effect of content and fineness. *Construction Building Materials, 128(5),* 361–372. DOI 10.1016/j.conbuildmat.2016.10.031.
30. Wang, C. L., Ni, W., Zhang, S. Q., Wang, S., Gai, G. S. (2016). Preparation and properties of autoclaved aerated concrete using coal gangue and iron ore tailings. *Construction Building Materials, 104,* 109–115. DOI 10.1016/j.conbuildmat.2015.12.041.
31. Yang, J., Hu, H., He, X., Su, Y., Pan, H. J. C. et al. (2021). Effect of steam curing on compressive strength and microstructure of high volume ultrafine fly ash cement mortar. *Construction and Building Materials, 266(5),* 120894. DOI 10.1016/j.conbuildmat.2020.120894.
32. Zou, J., Guo, C., Zhou, X., Sun, Y., Yang, Z. J. C. et al. (2018). Sorption capacity and mechanism of Cr^{3+} on tobermorite derived from fly ash acid residue and carbide slag. *Colloids and Surfaces A: Physicochemical and Engineering Aspects, 538,* 825–833. DOI 10.1016/j.colsurfa.2017.11.073.
33. Wang, Y., Zheng, T., Zheng, X., Liu, Y., Darkwa, J. et al. (2020). Thermo-mechanical and moisture absorption properties of fly ash-based lightweight geopolymer concrete reinforced by polypropylene fibers. *Construction and Building Materials, 251(8),* 118960. DOI 10.1016/j.conbuildmat.2020.118960.
34. Rustamov, S., Woo Kim, S., Kwon, M., Kim, J. (2021). Mechanical behavior of fiber-reinforced lightweight concrete subjected to repeated freezing and thawing. *Construction and Building Materials, 273(9),* 121710. DOI 10.1016/j.conbuildmat.2020.121710.
35. Zhu, C., Niu, J., Li, J., Wan, C., Peng, J. (2017). Effect of aggregate saturation degree on the freeze-thaw resistance of high performance polypropylene fiber lightweight aggregate concrete. *Construction and Building Materials, 145(7),* 367–375. DOI 10.1016/j.conbuildmat.2017.04.039.
36. Gyurkó, Z., Jankus, B., Fenyvesi, O., Nemes, R. (2019). Sustainable applications for utilization the construction waste of aerated concrete. *Journal of Cleaner Production, 230(2),* 430–444. DOI 10.1016/j.jclepro.2019.04.357.
37. Gong, J., Zhang, W. (2019). The effects of pozzolanic powder on foam concrete pore structure and frost resistance. *Construction and Building Materials, 208(76),* 135–143. DOI 10.1016/j.conbuildmat.2019.02.021.
38. Solid Waste. Extraction Procedure for Leaching Toxicity. Horizontal Vibration Method (2010). HJ 557-2010 C.F.R.
39. Determination of 34 Elements (Pb,Cd,V,P etc.). Inductively Coupled Plasma Mass Spectroscopy (ICP-MS) (2007). SL 394.2-2007 C.F.R.
40. Kurama, H., Karakurt, C. (2009). Properties of the autoclaved aerated concrete produced from coal bottom ash. *Journal of Materials Processing Technology, 209(2),* 767–773. DOI 10.1016/j.jmatprotec.2008.02.044.
41. Schreiner, J., Jansen, D., Ectors, D., Goetz-Neunhoeffer, F., Neubauer, J. et al. (2018). New analytical possibilities for monitoring the phase development during the production of autoclaved aerated concrete. *Cement and Concrete Research, 107(S1),* 247–252. DOI 10.1016/j.cemconres.2018.02.028.